

## RESEARCH ARTICLE

# Successive Ionic Layer Adsorption and Reaction (SILAR) Synthesis of CoMoO<sub>4</sub> Nanostructures for High-Performance Supercapacitors: Structural and Electrochemical Characterization

Avdhut Sutar<sup>1</sup>, Jayshree Patil<sup>1</sup>, Tejaswini Yadav<sup>3</sup>, Shamal Shingte<sup>2</sup>, Prashant B. Patil<sup>2</sup>, Sachin Pawar<sup>1,\*</sup>

**ABSTRACT:** Supercapacitors have emerged as promising energy storage devices due to their high power density and rapid charge-discharge capabilities. In this work, we report the facile and scalable synthesis of cobalt molybdate (CoMoO<sub>4</sub>) nanostructures using the Successive Ionic Layer Adsorption and Reaction (SILAR) method, an eco-friendly and cost-effective deposition technique. The structural, morphological, and electrochemical properties of as-deposited CoMoO<sub>4</sub> on Ni-foam and its annealed counterpart (CM300, treated at 300°C for 4 hours) were systematically investigated. X-ray diffraction (XRD) confirmed the crystalline phase of CoMoO<sub>4</sub>, while scanning electron microscopy (SEM) revealed a nanostructured morphology that enhances active surface area for electrochemical reactions. Electrochemical evaluations, including cyclic voltammetry (CV) and galvanostatic charge-discharge (GCD) measurements in a 2 M KOH electrolyte, demonstrated outstanding supercapacitive performance. The CM300 electrode exhibited a remarkable specific capacitance of 1126 F g<sup>-1</sup> at 5 mA cm<sup>-2</sup>, along with a high energy density of 56.34 Wh kg<sup>-1</sup> and a power density of 340.9 W kg<sup>-1</sup>. The enhanced performance is attributed to the improved crystallinity and porous nanostructure of the annealed CoMoO<sub>4</sub>, facilitating efficient ion diffusion and charge transfer. Additionally, the binder-free electrode fabrication on Ni-foam enhances mechanical stability and practical applicability for supercapacitor devices. This study highlights the potential of SILAR-synthesized CoMoO<sub>4</sub> as a high-performance electrode material for next-generation supercapacitors, offering a sustainable and scalable approach for energy storage applications.

**Keywords:** Cobalt molybdate (CoMoO<sub>4</sub>), SILAR method, Supercapacitor, Nanostructured electrodes, Energy storage.

Received: 16 September 2024; Revised: 12 November 2024; Accepted: 24 January 2025; Published Online: 21 February 2025

## 1. INTRODUCTION

Supercapacitors are emerging as highly efficient and versatile energy storage systems. They are positioned as a promising alternative to lithium-ion batteries due to their superior

power density and rapid charge-discharge capabilities [1]. With their remarkable ability to deliver high power compared to batteries, supercapacitors play a pivotal role in meeting the growing energy demands of compact consumer electronics, electric vehicles, laptops, small electronic wearable gadgets, and devices requiring swift energy delivery [2]. Supercapacitors are categorized into two distinct types based on their charge storage mechanism. The first type is electrical double-layer capacitors (EDLCs), which store charge at the interface. The second type, pseudocapacitor, relies on faradaic reactions occurring at the electrode/electrolyte interface for charge storage. While pseudocapacitors exhibit higher energy storage capacity than EDLCs, they face challenges such as limited cyclic stability. Since the charge

<sup>1</sup> Shri Vijaysinha Yadav College, Peth Vadgaon, District Kolhapur (Affiliated to Shivaji University Kolhapur), Maharashtra-416112, India.

<sup>2</sup> Department of Physics, The New College, Kolhapur (Affiliated to Shivaji University Kolhapur), Maharashtra-416012, India.

<sup>3</sup> V N & B N Mahavidyalaya, Shirala, District Sangli, (Affiliated to Shivaji University Kolhapur), Maharashtra-415408, India.

\* Author to whom correspondence should be addressed:  
[asachinpawar@gmail.com](mailto:asachinpawar@gmail.com) (Sachin Pawar)

storage performance of pseudocapacitors is mainly influenced by the redox processes at the electrode/electrolyte interface, their efficiency can be significantly enhanced by utilizing nanostructured redox-active materials [3-5]. Carbon-based materials, such as carbon nanotubes (CNTs), graphene, and their derivatives, serve as electrode materials in electric double-layer capacitors (EDLCs). In contrast, electrodes based on transition metal oxides and hydroxides are predominantly used in pseudocapacitors [6-7].

Among the different types of supercapacitors, pseudocapacitive have garnered significant attention due to their excellent energy and power density compared with EDLCs. This has led researchers to focus on developing pseudocapacitive materials to achieve higher energy storage capability [8]. Also, recent studies on pseudocapacitive materials, such as polymer-based materials like polyacetylene, polyaniline, polyfluorene, etc, have gained more interest in energy storage applications. These materials exhibit exceptional flexibility and strong adhesion properties, making them a promising candidate in supercapacitor applications [9-10]. Moreover, the transition metal sulfides and phosphides have also been widely studied due to their excellent thermal stability and electrical conductivity. However, synthesizing metal sulfides and phosphides involves a toxic procedure, prompting researchers to seek a non-toxic, simple, and cheaper choice for energy storage systems [11-12]. In this regard, transition metal oxides (TMOs) have emerged as a prominent class of materials due to their affordability, abundance, and environmentally friendly characteristics. In the last decades, different TMOs, such as NiO, MoO<sub>3</sub>, CuO, MnO<sub>2</sub>, RuO<sub>2</sub>, Co<sub>3</sub>O<sub>4</sub>, and TiO<sub>2</sub>, with diverse morphologies and structures, have been extensively studied [13]. Most studies have expanded research on TMOs to include binary, ternary, and multicomponent oxides, exhibiting enhanced electronic structures and excellent chemical, physical, and electrochemical properties [14-15]. Incorporating multiple metal components in TMOs has demonstrated a significant advantage in electrochemical performance and electrical conductivity compared to single metal oxides [16]. As a result, extensive research efforts have been directed towards metal molybdates (e.g., CoMoO<sub>4</sub>, NiMoO<sub>4</sub>, and MnMoO<sub>4</sub>) to improve electrode performance in supercapacitor applications due to their abundance, low cost and the reliable redox transformations [17-18]. In this scenario, metal molybdates have been intensively attracted as a prominent agent among other TMOs due to their different multidisciplinary applications, such as electrochemical sensors, photoluminescence, photocatalysis, and energy storage [13].

Recently, Zhuoxun Yin, et al. synthesized NiMoO<sub>4</sub> nanotubes using a hydrothermal method and obtained a specific capacitance of 864 F g<sup>-1</sup> at the current density of 1 A g<sup>-1</sup> [19]. In another report, Veerasubramani et al. prepared CoMoO<sub>4</sub> and showed the capacitance of 133 F g<sup>-1</sup> at 1 mA cm<sup>-2</sup> [20]. Gao et al. synthesized a micro flower-like morphology of ZnMoO<sub>4</sub> and obtained the maximum capacitance value of 704 F g<sup>-1</sup> at 1 A g<sup>-1</sup> [21]. Also, Cai et al.

synthesized nanospheres of NiMoO<sub>4</sub> and obtained an excellent specific capacitance of 974 F g<sup>-1</sup> at 1 A g<sup>-1</sup> [22]. In other ways, Ge et al. prepared a CoMoO<sub>4</sub>/Co<sub>1-x</sub>S binary composite via a two-step hydrothermal method for supercapacitor application, which exhibited a maximum specific capacitance of 2250 F g<sup>-1</sup> at a current density of 1 A g<sup>-1</sup> [23]. Zhang et al. prepared NiMoO<sub>4</sub>@CoMoO<sub>4</sub> hierarchical nanospheres anchored on nickel foam using the hydrothermal method and reported a high specific capacitance of 1601.6 F g<sup>-1</sup> at a current density of 2 A g<sup>-1</sup> [24]. Zhuoxun et al. developed a hierarchical nanosheet-based CoMoO<sub>4</sub>@NiMoO<sub>4</sub> nanotubes using a hydrothermal approach. They achieved a specific capacitance of 1079 F g<sup>-1</sup> at a current density of 5 A g<sup>-1</sup> with 98.4% capacitance retention after 1000 cycles [25].

This report presents the successive ionic layer adsorption and reaction (SILAR) method for depositing both as-prepared and annealed CoMoO<sub>4</sub> on Ni-foam substrates for supercapacitor applications. The structural, morphological, and electrochemical properties of the as-prepared and annealed CoMoO<sub>4</sub> on Ni-foam were systematically investigated using X-ray Diffraction (XRD) and Scanning Electron Microscopy (SEM). The electrochemical performance of the CoMoO<sub>4</sub> on Ni-foam was studied using cyclic voltammetry (CV) and galvanostatic charge-discharge (GCD) measurements in a 2 M KOH electrolyte. These results depict that the SILAR deposited CoMoO<sub>4</sub> on Ni-foam (CM300) shows excellent specific capacitance of 1126 F g<sup>-1</sup> at a current density of 5 mA cm<sup>-2</sup>, along with a power density of 340.9 W kg<sup>-1</sup> and an energy density of 56.34 W h kg<sup>-1</sup>. These findings highlight the potential of SILAR-deposited CoMoO<sub>4</sub> on Ni-foam as a high-performance electrode material for next-generation supercapacitors.

## 2. EXPERIMENTAL DETAILS

### 2.1. Materials and Reagents

All analytical grade (AR) chemicals were used without further purification, and all solutions were prepared using double-distilled water (DDW). Cobalt (III) chloride hexahydrate (CoCl<sub>2</sub>.6H<sub>2</sub>O, 98%), sodium molybdate (Na<sub>2</sub>MoO<sub>4</sub>.2H<sub>2</sub>O, 98%) were purchased from Loba Chemie Pvt Ltd. and Potassium hydroxide (KOH, 98%) was utilized as the electrolyte for electrochemical tests.

### 2.2. Synthesis of CoMoO<sub>4</sub> on Ni-foam

In the present work, nickel foam (Ni foam) was used as a substrate for depositing CoMoO<sub>4</sub> samples through successive ionic layer adsorption and reaction (SILAR). The Ni foam substrate was initially cleaned with DDW. The process consists of ultrasonic cleaning in ethanol for 15 minutes to remove organic/chemical impurities, which is further followed by immersion in 0.5 M HCl for 10 minutes to

eliminate the surface oxides. Then, the foam is rinsed thoroughly with the DDW to remove the residual acid. Finally, it was dried in air at room temperature. A cobalt chloride (CoCl<sub>2</sub>·6H<sub>2</sub>O) and sodium molybdate (Na<sub>2</sub>MoO<sub>4</sub>) were used as a cationic and anionic precursor solution for the SILAR process, respectively. To prepare the cationic precursor solution, 0.3 M cobalt chloride (CoCl<sub>2</sub>·6H<sub>2</sub>O) was dissolved in 50 mL of distilled water. In contrast, for the anionic precursor solution, 0.1 M sodium molybdate (Na<sub>2</sub>MoO<sub>4</sub>) was dissolved in 50 mL of distilled water. Each precursor solution was then magnetically stirred for 30 minutes to form a homogeneous solution. Depositing the CoMoO<sub>4</sub> thin films on Ni foam by SILAR method consists of four steps in a cycle; in the first step, the Ni substrate was initially immersed into the cobalt chloride solution for 20 s for the process of absorption, and the Co<sup>+</sup> ions will be chemically adsorbed to the surface of the substrate. In the second step, the substrate was again dipped into the DDW for the rinsing process and to remove the loosely bounded and un-adsorbed ions on the surface of the substrate. In the third step, the substrate was again immersed into the sodium molybdate for 20 s for a reaction process in which the adsorbed ions will react with MoO<sub>4</sub><sup>-</sup> ions on the substrate surface. In the fourth step, the Ni substrate was taken out and again rinsed with deionized water to remove the unreacted ions and precursor solution. The thickness of the films was optimized by controlling and increasing the number of deposition cycles, respectively. Furthermore, CoMoO<sub>4</sub> deposited on Ni-foam at room temperature is designated as 'CM-RT' while the annealed CoMoO<sub>4</sub> on Ni-foam, treated at 300 °C for 4 hours, is labelled as 'CM300'. Figure 1 represents the schematic illustration of the synthesis procedure of CoMoO<sub>4</sub> on Ni-foam.

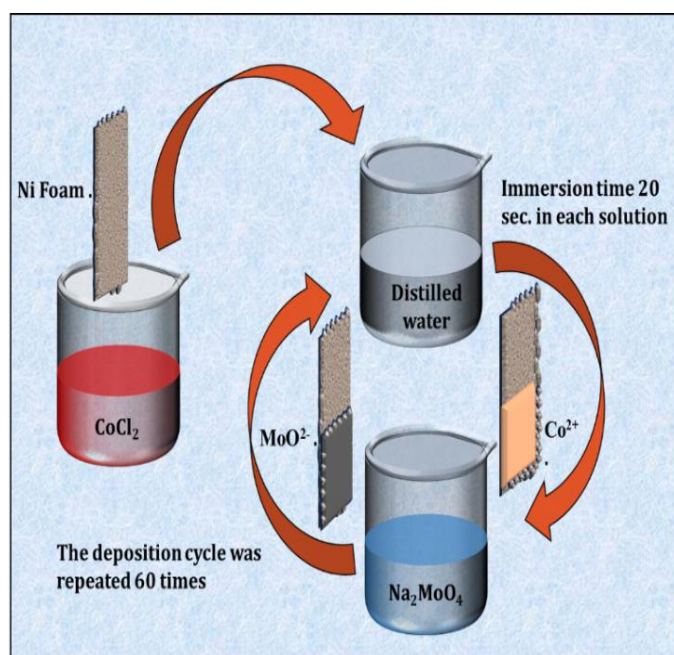


**Fig. 1.** Schematic showing preparation of CoMoO<sub>4</sub> on Ni-foam.

## 2.3. Material Characterizations

The phase and purity of both as-prepared and annealed CoMoO<sub>4</sub> thin films were characterized using X-ray diffraction (XRD, Rigaku, Smart Lab) with CuK $\alpha$  radiation ( $\lambda = 1.54 \text{ \AA}$ ). Field emission scanning electron microscopy (FE-SEM, JSM-7800F, JEOL, Japan), coupled with energy dispersive X-ray spectroscopy (EDS; Oxford, X-Max), was employed to analyze the surface morphology.

## 2.4. Electrochemical measurements

Various electrochemical analysis techniques, such as cyclic voltammetry (CV), galvanostatic charge-discharge (GCD), and electrochemical impedance spectroscopy (EIS), were employed to investigate the electrochemical properties of CoMoO<sub>4</sub> thin films. These analysis were conducted on both as-fabricated samples and those subjected to annealing at 300 °C for 4 hours. The electrochemical studies of these electrodes were performed using a standard three-electrode system in an electrolyte solution of 2 M KOH, with an Ag/AgCl electrode serving as the reference electrode and a platinum wire as the counter electrode. The electrochemical analysis equations are mentioned below.

The specific capacitance of the thin film was extracted from the CV and GCD curves by employing the following equations.

Specific capacitance from CV:

$$C_s = \frac{1}{m \cdot v(v_2 - v_1)} \int_{v_1}^{v_2} I v dv \quad (1)$$

where,  $I$  represent the current density ( $\text{mA cm}^{-2}$ ),  $v$  is the scan rate ( $\text{mV s}^{-1}$ ), and  $(v_2 - v_1)$  is the working potential window and the specific capacitance ( $C_s$ ), areal capacitance ( $C_a$ ).

Aerial capacitance from CV:

$$C_a = \frac{1}{v(v_2 - v_1)} \int_{v_1}^{v_2} I v dv \quad (2)$$

Specific capacitance from GCD:

$$C_s = \frac{I \times \Delta t}{m \times \Delta v} \quad (3)$$

where  $I$  is the current (mA),  $\Delta t$  is the discharge time (s),  $m$  is the active mass of thin film (gm),  $\Delta v$  is the potential window (Volt).

Aerial capacitance from GCD:

$$C_a = \frac{I \times \Delta t}{\Delta v} \quad (4)$$

Also, energy density  $E$  ( $\text{Wh kg}^{-1}$ ) and power density  $P$  ( $\text{W kg}^{-1}$ ) were calculated from the GCD curve with the following equations

$$E = \frac{0.5 \times C \times (v_2 - v_1)^2}{3.6} \quad (5)$$

$$P = \frac{E \times 3600}{\Delta t} \quad (6)$$

### 3. RESULTS AND DISCUSSION

#### 3.1. Characterization

##### 3.1. Structural analysis

X-ray diffraction (XRD) analysis was carried out to examine the phase composition and crystal structure of CM-RT and CM300. The XRD pattern of CM300 (Figure 2 (a)) indicates a noticeable crystallinity enhancement compared to CM-RT (Figure 2 (b)). The CM-RT did not exhibit distinct CoMoO<sub>4</sub> diffraction peaks, likely due to the predominant signal from the Ni-foam substrate. However, as the sample annealed at a particular annealing temperature of 300 °C, the intensity of the CoMoO<sub>4</sub> peaks progressively strengthened, which signified improved crystal growth. The diffraction peaks detected in CM300 at 19.05°, 23.40°, 26.52°, and 58.42° correspond to the (-201), (021), (002) and (024) planes of the monoclinic CoMoO<sub>4</sub> respectively. These peak positions align well with the indexed reference pattern (JCPDS No. 21-0868) [26-27]. Thus, it confirms the successful phase formation of CoMoO<sub>4</sub> onto the Ni-foam substrate at 300 °C.

##### 3.2. Morphological analysis

The surface morphology of CM-RT and CM300 on Ni-foam

was analyzed using scanning electron microscopy (SEM). This gives a crucial insight into the material's structural characteristics and potential electrochemical performance. Figure 3 shows the low and high-magnification views of CM-RT and CM300 on Ni-foam. Figures 3 (a) and (b) reveal the incomplete or suboptimal growth of the material, while Figures 3 (c) and (d) represent the distinct transformation towards nanofiber morphology. The transformation of such morphological change reveals that the annealing process can facilitate the material's alignment and elongation, increasing the surface area and structural integrity [28-30]. The nanofiber's morphology, characterized by its elongated structure and improvement in crystallinity, can significantly affect the electrochemical properties utilized for supercapacitor application [31].

##### 3.3. Elemental analysis

Energy Dispersive X-ray Spectroscopy (EDAX) was employed to study the elemental analysis CoMoO<sub>4</sub> deposited on a Nickel foam. The EDAX spectrum (Figure 4) confirmed the existence of Cobalt (Co), Molybdenum (Mo), and Oxygen (O), verifying the successful formation of the CoMoO<sub>4</sub> material. The atomic weight percentages, determined by quantitative analysis and presented in Table 1, are Co (25.80 %), Mo (21.14 %), and O (53.07 %). The observed weight percentages reflect the relative abundance of each element in the CoMoO<sub>4</sub> structure.

**Table 1.** Elemental composition of CM300 on Ni-foam.

Element	Atomic weight (%)
Co	25.80
Mo	21.14
O	53.07

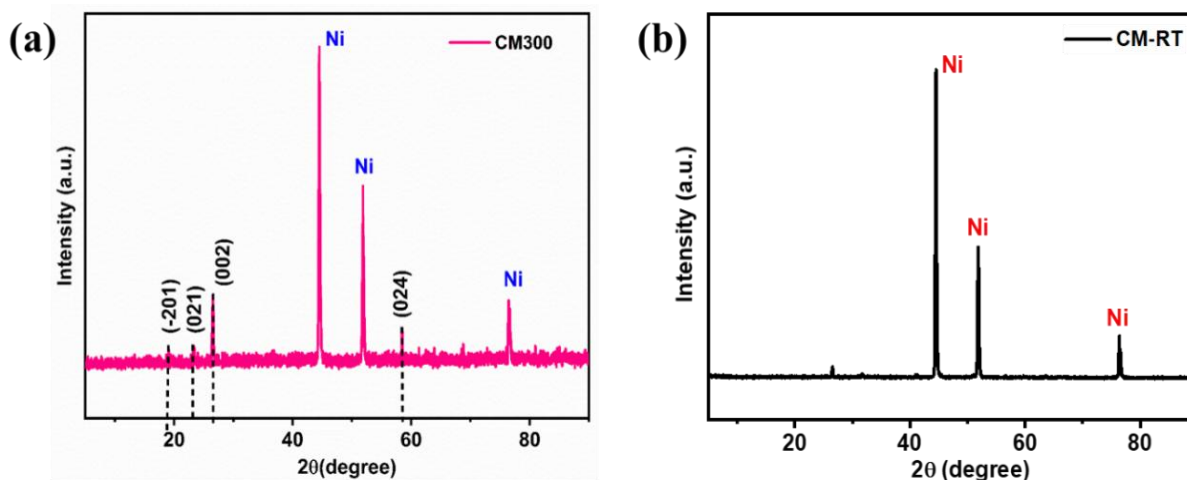


**Fig. 2.** XRD patterns of (a) CM300 and (b) CM-RT on Ni-foam.

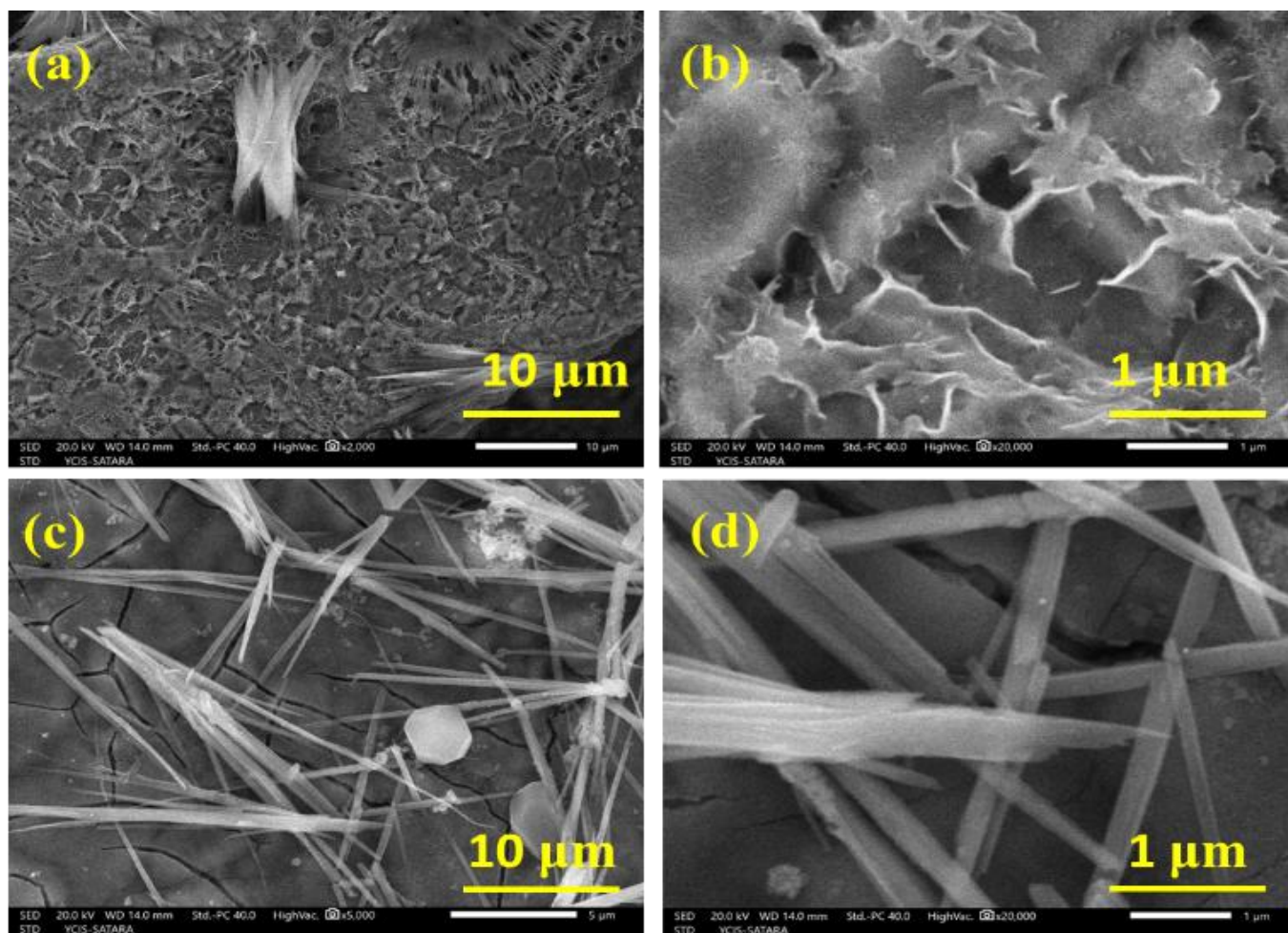


**Fig. 3.** SEM images of (a-b) CM-RT and (c-d) CM300 on Ni-foam.

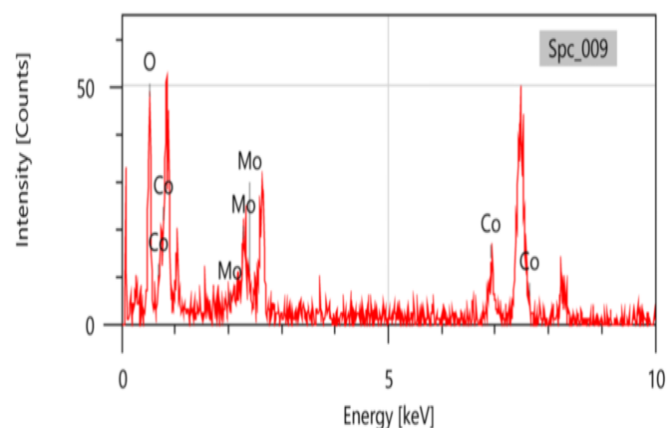


**Fig. 4.** EDAX pattern of CM300 on Ni-foam.

### 3.4. Electrochemical performance of CoMoO<sub>4</sub> on Ni-foam

The electrochemical behavior of both as-synthesized and annealed CoMoO<sub>4</sub> on Ni-foam was evaluated using cyclic voltammetry (CV) in a 2 M aqueous KOH electrolyte

solution, as illustrated in Figure 5. Notably, the aqueous KOH was chosen as the optimal electrolyte for CoMoO<sub>4</sub> deposited on Ni-foam as electrode material in supercapacitor applications due to its high ionic conductivity, broad electrochemical stability window, and enhanced pseudocapacitive behavior.

Also, it provides a low pH environment, minimizes corrosion, enhances safety, and improves overall electrochemical performance. The comparative analysis of the CM-RT and CM300 at a scan rate of 10 mV s<sup>-1</sup> is represented in Figure 5 (a). The operating potential window for the CoMoO<sub>4</sub> on Ni-foam is approximately 0 to 0.6 V (vs Ag/AgCl) in a 2 M KOH aqueous electrolyte, which is well-suited for facilitating the faradaic redox transitions in the CoMoO<sub>4</sub> electrode material. The CV profiles show that samples have distinctive reduction-oxidation peaks demonstrating pseudocapacitive behavior controlled by faradaic processes [32]. The observed redox pair of peaks is due to the charge transfer kinetics mechanism of the Co<sup>2+</sup> into the Co<sup>3+</sup> in the CM300 on Ni-foam [33]. At a low scan rate of 10 mV s<sup>-1</sup>, an anodic peak appears at 0.47 V, corresponding to the oxidation process. In contrast, a cathodic peak around 0.24 V, associated with the reduction process is observed.

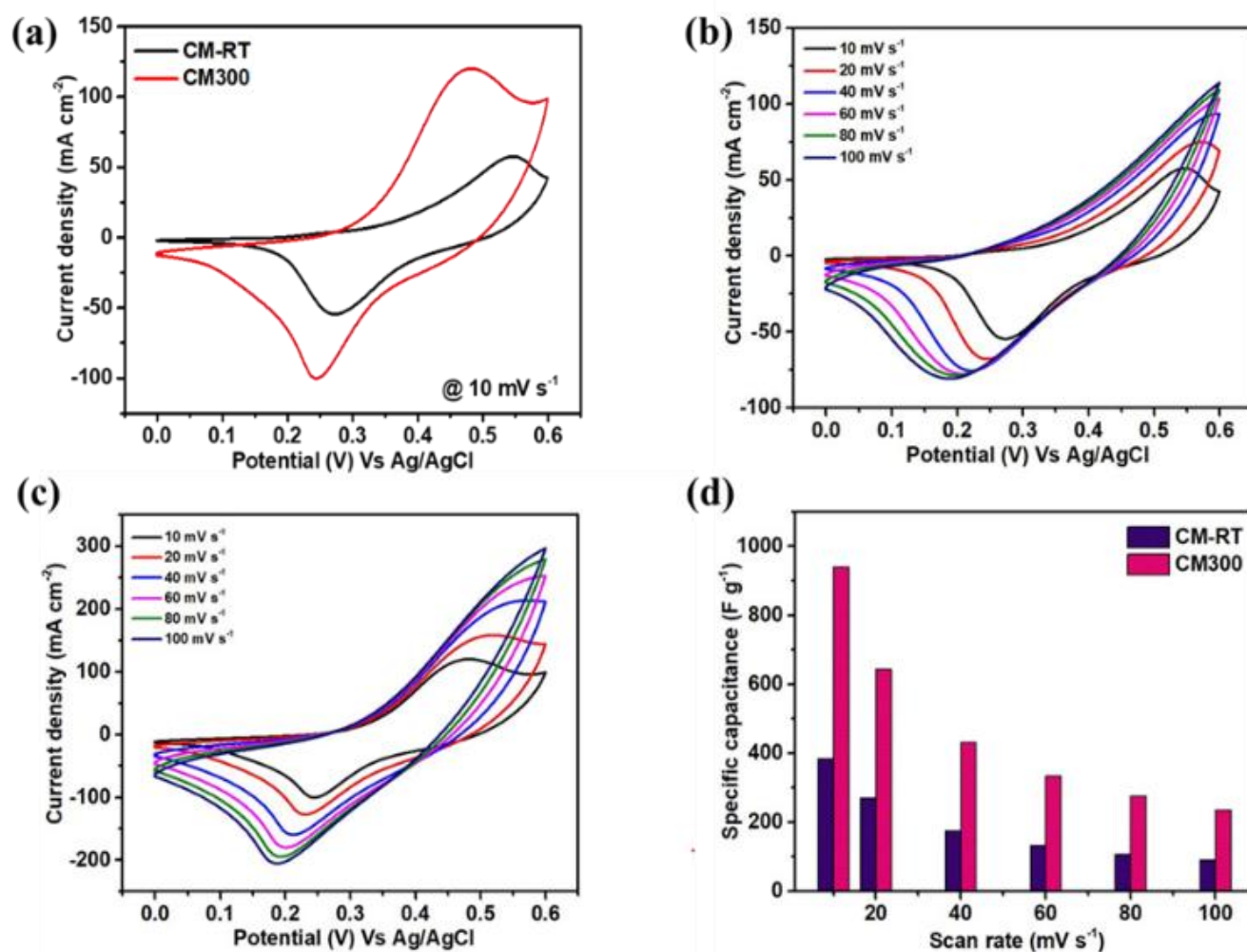


**Fig. 5.** (a) CV curves for CM-RT and CM300 at a fixed scan rate of 10 mV s<sup>-1</sup>; CV curves for (b) CM-RT; (c) CM300 at different scan rates ranging from 10 to 100 mV s<sup>-1</sup>; and (d) Specific capacitance value as a function of scan rate.

Further, to investigate the insight, the pseudocapacitive behavior of the CoMoO<sub>4</sub> sample and CV curves of CM-RT and CM300 are recorded at different scan rates ranging from 10 to 100 mV s<sup>-1</sup> (Figure 5 (b) and (c)). With increasing scan rates, the CM300 on Ni-foam exhibited redox peak shifts, which can be analyzed to determine the degree of electrochemical reversibility. At higher scan rates, the anodic cathodic peaks shift to more positive and negative potentials, respectively, implying that charge transfer kinetics may be the rate-limiting step.

In addition, the overall shape of the CV profiles remains unchanged as the scan rate increases, suggesting an improvement in mass transport and electron conduction inside the material. The areal capacitance and specific capacitance of the CoMoO<sub>4</sub> on Ni-foam at different scan rates were extracted from CV curves using equations (1) and (2). Figure 5 (d) shows the graph of the specific capacitance value of CM-RT and CM300 as a function of scan rate. The CM300 sample exhibited a specific capacitance of 939.22 F g<sup>-1</sup> at a scan rate of 10 mV s<sup>-1</sup>. Notably, even at a high scan rate of 100 mV s<sup>-1</sup>, the sample maintained a commendable specific capacitance of 235.39 F g<sup>-1</sup>. Furthermore, Figure 6

(a) shows the effect of scan rate on the specific capacitance and areal capacitance of CM300. Figure 6 (b) demonstrates a linear relationship between peak current density and the square root of scan rates, indicating enhanced electrochemically reversible redox reactions and efficient electronic and ionic transport within the CM300 on Ni-foam.

In addition, galvanostatic charge-discharge (GCD) evaluations were further performed in the potential range from 0 to 0.6 V (vs Ag/AgCl) at different current densities to extract the specific capacitance and areal capacitance of the materials. Figure 7 (a) compares the GCD curves CM-RT and CM300 at the fixed current density of 5 mA cm<sup>-2</sup>. The observed distinct plateau-like regimes (non-linear profiles) suggest the faradaic behavior of the CM-RT and CM300, which is in very correlation with CV curve (Figure 5 (b) and (c)). Figure 7 (b) shows the GCD profile of the CM-RT at current densities ranging from 5 to 25 mA cm<sup>-2</sup>. Similarly, the GCD curves for CM300 densities are shown in Figure 7 (c). The CM300 depicts rapid charging/discharging at higher current density, whereas, at low current density, it represents a better charging/discharging profile.

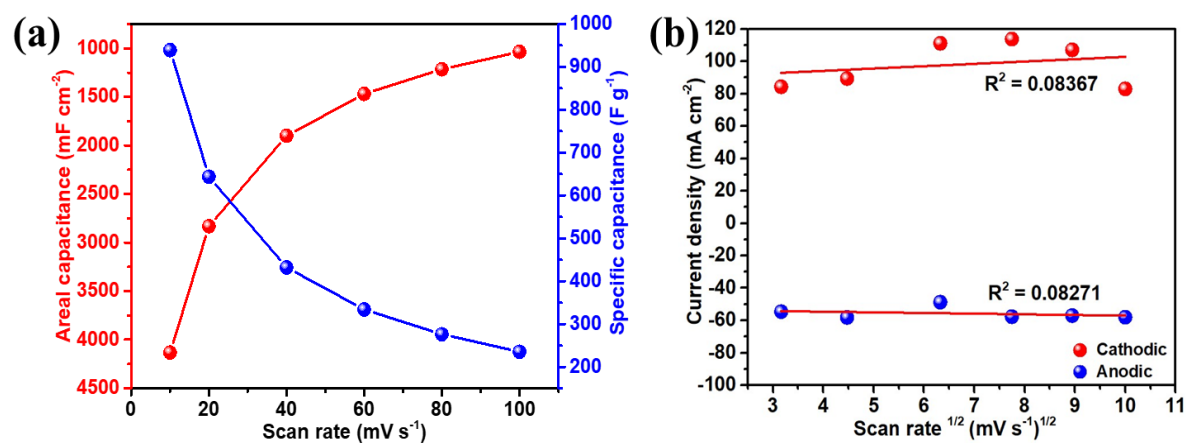


**Fig. 6.** (a) Effect of scan rate on the specific capacitance and areal capacitance of CM300; (b) Linear relationship of the peak current density (anodic and cathodic) against the square root of scan rates.

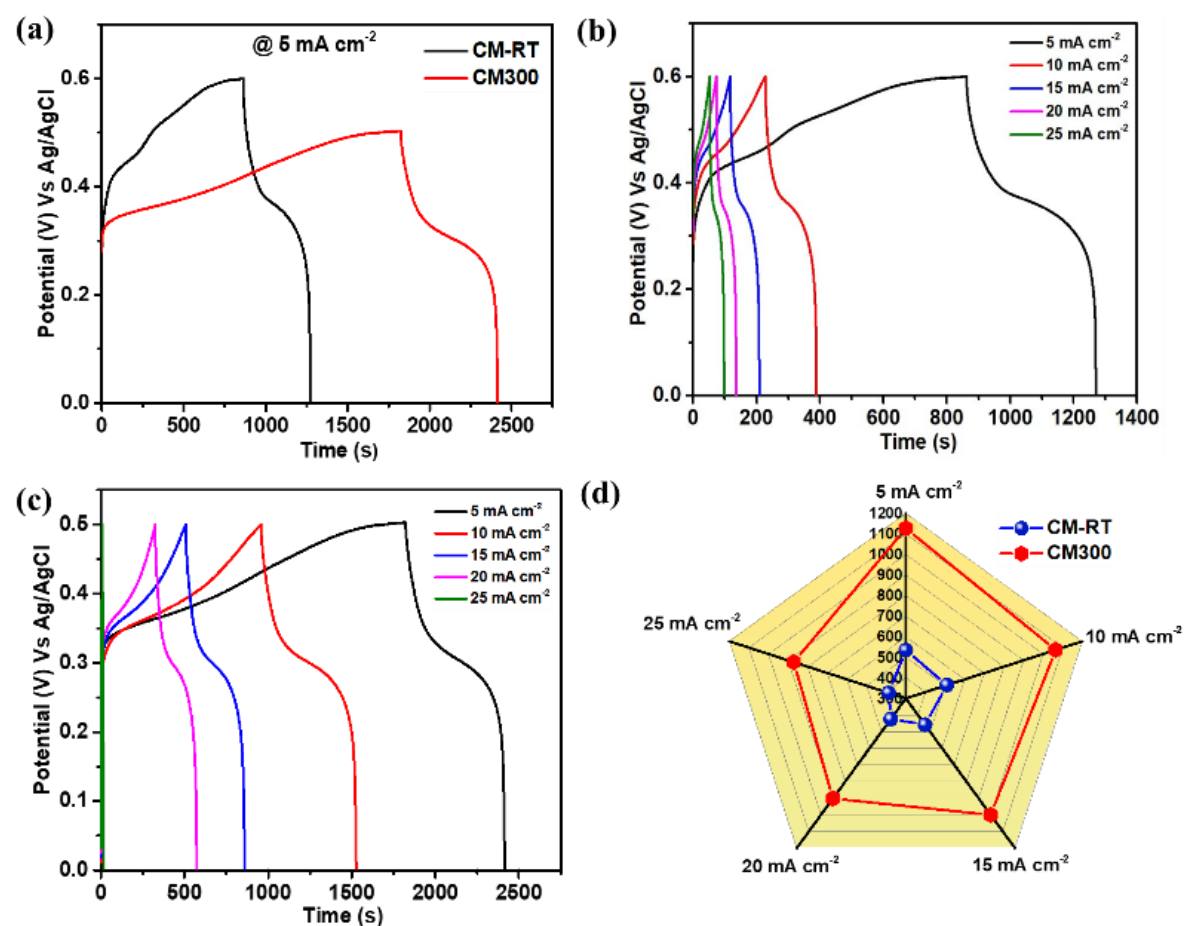


**Fig. 7.** (a) GCD curves for CM-RT and CM300 on Ni-foam at a fixed current density of 5  $\text{mA cm}^{-2}$ ; GCD curves for (b) CM-RT; (c) CM300 on Ni-foam at different current densities ranging from 5 to 25  $\text{mA cm}^{-2}$ ; and (d) Radar plot depicting the specific capacitance values of CM-RT and CM300 as a function of current density.

The specific capacitance of CM-RT and CM300 was calculated from the discharge time using the equation (3). CM300 delivers the specific capacitance as 1126, 1064, 1000, 902, and 871  $\text{F g}^{-1}$  at a current density of 5, 10, 15, 20, and

25  $\text{mA cm}^{-2}$ , respectively. Figure 7(d) displays the Radar plot depicting the specific capacitance values of CM-RT and CM300 as a function of current density. It demonstrates that the CM300 on Ni foam can possess an excellent specific

capacitance of 1126 F g<sup>-1</sup> at a current density of 5 mA cm<sup>-2</sup> compared to the CM-RT.

The obtained maximum specific capacitance at lower current density is due to the controlled mass transfer of the electrolytic ions into the internal region of the electrode material

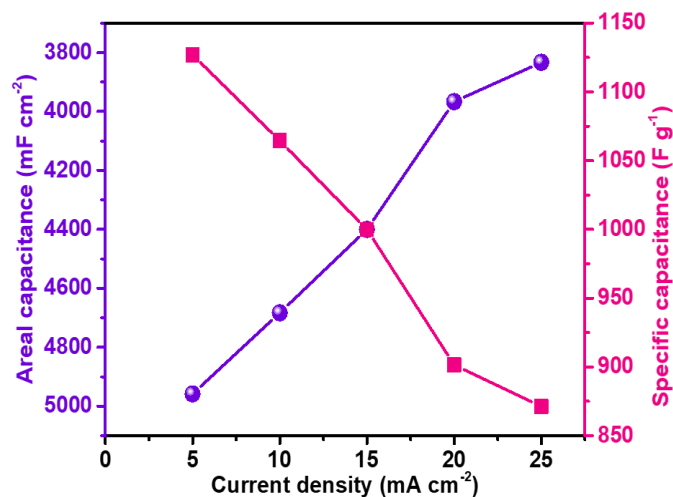


**Fig. 8.** Effect of different current densities on the specific capacitance and areal capacitance of CM300.

Furthermore, Figure 8 shows the effect of current densities on the specific capacitance and areal capacitance of CM300 calculated from GCD curves using equations (3) and (4). The specific capacitance of CM300 was compared to the capacitance values of reported materials (Figure 9).

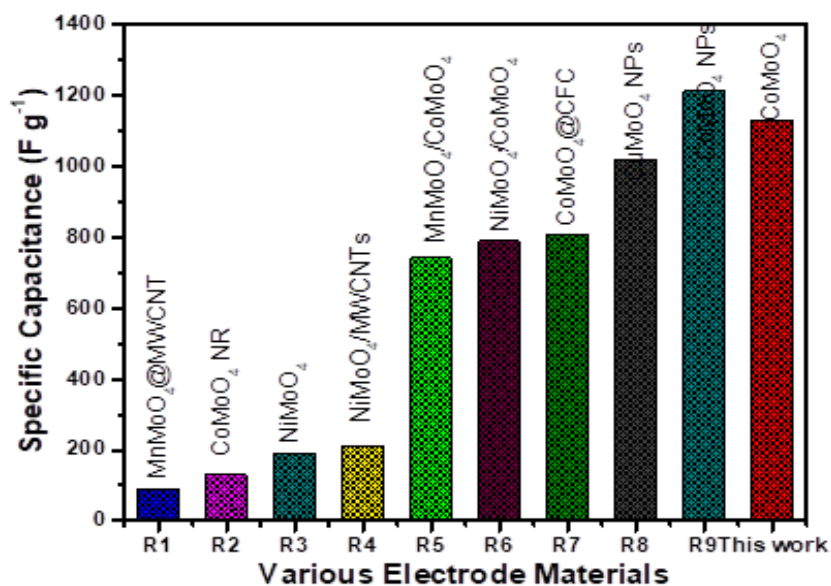
The energy density and power density of the CM300 are calculated using the equations (5) and (6). The computed power densities of CM300 were 340.9, 681.8, 1022, 1363, and 1704 W kg<sup>-1</sup>, at energy densities of 56.34, 53.21, 50,

45.07, and 43.56 W h kg<sup>-1</sup>. The CoMoO<sub>4</sub> (CM300) on the Ni-foam electrode demonstrates a peak power density of 340 W kg<sup>-1</sup> and an energy density of 56.34 W h kg<sup>-1</sup> at 5 mA cm<sup>-2</sup>. The comparative study of the electrochemical properties of the CM300 with the other reported electrode materials is given in Table 2.

The electrochemical impedance spectroscopy (EIS) was employed to analyze the ion transport behavior and charge storage dynamics of the CoMoO<sub>4</sub> on Ni-foam electrode in a 2 M aqueous KOH electrolyte solution. The EIS measurements were performed across a wide frequency range, from 1000 KHz to 1 Hz, using an AC potential of about 5 mV. This characterization technique provides more critical insights into the electrode's capacitive and resistive features, which can play a key role in performing its electrochemical behavior. The Nyquist plot, depicted in Figure 10, features a semicircle in the high-frequency region and a linear segment at lower frequencies.

A small semicircle at high frequencies can signify a charge transfer resistance ( $R_{ct}$ ), while the linear part in the low-frequency region reflects ion diffusion behavior within the electrode material. Also, the equivalent series resistance ( $R_s$ ), which represents the total resistance of the electrolyte, intrinsic resistance of the electrode material, the current collector, and the electrode/current collector interface, was determined as 1.39  $\Omega$ .

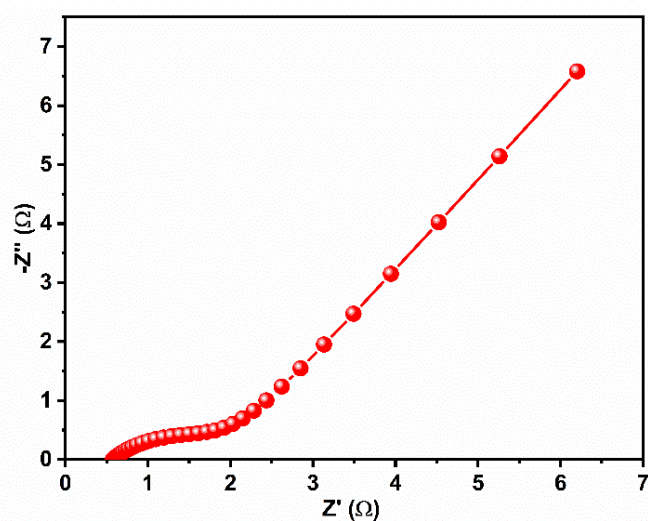
The low  $R_s$  value signifies efficient charge transport and minimal ohmic losses, which are essential for high-performance energy storage applications. The  $R_{ct}$  derived from the obtained semicircle diameter in the high-frequency region was 1.62  $\Omega$ . This relatively low value of  $R_{ct}$  demonstrates an efficient charge transfer process between the CM300 material and electrolyte, improving the electrochemical reaction kinetics. The electron and ion transport enhancement at the electrode material-electrolyte interface facilitates a rapid redox reaction, a key mechanism in pseudocapacitive charge storage.



**Fig. 9.** Comparative study of prepared electrode material (CM300) with the other electrode materials.

**Table 2.** Comparative study of specific capacitance of prepared electrode material (CM300) with the other reported electrode materials.

Sr. No.	Material	Electrolyte	Specific Capacitance (Fg <sup>-1</sup> )	Ref. No.
1	MnMoO <sub>4</sub> @MWCNT	1 M KOH	1017 at 1 A g <sup>-1</sup>	32
2	CoMoO <sub>4</sub> NR	1 M KOH	89.5 at 1 mA cm <sup>-2</sup>	34
3	NiMoO <sub>4</sub>	1 M KOH	740 at 1 A g <sup>-1</sup>	35
4	NiMoO <sub>4</sub> /carbon	1 M KOH	805 at 1 A g <sup>-1</sup>	36
5	MnMoO <sub>4</sub> /CoMoO <sub>4</sub>	2M NaOH	187 at 1 A g <sup>-1</sup>	37
6	NiMoO <sub>4</sub> /CoMoO <sub>4</sub>	1 M KOH	1445 at 1 A g <sup>-1</sup>	38
7	CoMoO <sub>4</sub> @CFC	3 M KOH	1210 at 2.5 A g <sup>-1</sup>	39
8	CuMoO <sub>4</sub> NPs	1 M KOH	127 at 1 mA cm <sup>-2</sup>	40
9	CoMoO <sub>4</sub> NPs	1 M KOH	1 F cm <sup>-2</sup>	41
10	CoMoO <sub>4</sub> on Ni foam	2 M KOH	1126 at 5 mA cm <sup>-2</sup>	<b>Present work</b>

**Fig. 10.** Nyquist plot of CM300 on Ni-foam.

#### 4. CONCLUSION

In this work, CoMoO<sub>4</sub> was successfully deposited on Ni-foam electrodes through the SILAR method. The resulting binder-free nanofiber structured material was used as an electrode for supercapacitor applications. Structural analysis confirmed the crystalline nature of the deposited CoMoO<sub>4</sub> with the monoclinic phase. SEM imaging revealed elongated, porous nanofibers morphology, facilitating efficient ion diffusion and charge storage. Electrochemical studies, including cyclic voltammetry and galvanostatic charge-discharge measurements, demonstrated excellent capacitive performance, with the CoMoO<sub>4</sub> annealed at 300°C for 4 hours (CM300) exhibiting a high specific capacitance of 1126 F g<sup>-1</sup> at a current density of 5 mA cm<sup>-2</sup>. Additionally, the CM300 electrode delivered a remarkable power density of 340.9 W kg<sup>-1</sup> and an energy density of 56.34 Wh kg<sup>-1</sup>, indicating its potential for high-performance energy storage applications. The enhanced electrochemical properties can be

attributed to the crystalline nature of CoMoO<sub>4</sub>, which improves active site accessibility and charge storage capabilities. The binder-free nature of the CoMoO<sub>4</sub> on Ni-foam electrodes enhances its practical applicability in supercapacitors by eliminating the need for additional binders or conductive additives, which often compromise electrochemical efficiency. These findings highlight the potential of the SILAR technique deposited CoMoO<sub>4</sub> on Ni-foam electrodes as promising candidates for next-generation supercapacitors. This study lays the groundwork for developing efficient, scalable, and sustainable energy storage solutions

#### DECLARATIONS

##### Ethical Approval

We affirm that this manuscript is an original work, has not been previously published, and is not currently under consideration for publication in any other journal or conference proceedings. All authors have reviewed and approved the manuscript, and the order of authorship has been mutually agreed upon.

##### Funding

Not applicable

##### Availability of data and material

All of the data obtained or analyzed during this study is included in the report that was submitted.

##### Conflicts of Interest

The authors declare that they have no financial or personal

interests that could have influenced the research and findings presented in this paper. The authors alone are responsible for the content and writing of this article.

### Authors' contributions

All authors contributed equally in the preparation of this manuscript.

### ACKNOWLEDGEMENTS

One of the authors, Dr. Sachin Pawar acknowledges financial support from Shivaji University Kolhapur under the "Diamond Jubilee Research Initiation Scheme".

### REFERENCE

- [1] Z.Y. Zhang, M.L. Liu, X. Tian, P. Xu, C.Y. Fu, S. Wang, Y.Q. Liu, **2018**. Scalable fabrication of ultrathin free-standing graphene nanomesh films for flexible ultrafast electrochemical capacitors with AC line-filtering performance. *Nano Energy* 50, pp.182–191.
- [2] H.M. El Sharkawy, A.S. Dhmees, A.R. Tamman, S.M. El Sabagh, R.M. Aboushabha, N.K. Allam, **2020**. N-doped carbon quantum dots boost the electrochemical supercapacitive performance and cyclic stability of MoS<sub>2</sub>. *Journal of Energy Storage* 27, pp.101078.
- [3] N. Ahmed, B.A. Ali, M. Ramadan, N.K. Allam, **2019**. Three-Dimensional interconnected binder-free Mn–Ni–S nanosheets for high performance asymmetric supercapacitor devices with exceptional cyclic stability. *ACS Applied Energy Materials*. 2, pp.3717–3725.
- [4] A.E. Elkholy, F. El-Taib Heikal, N.K. Allam, **2019**. A facile electrosynthesis approach of amorphous Mn–Co–Fe ternary hydroxides as binder-free active electrode materials for high-performance supercapacitors. *Electrochim. Acta*. 296, pp.59–68.
- [5] Umar, A., Ahmed, F., Ullah, N., Ansari, S.A., Hussain, S., Ibrahim, A.A., Qasem, H., Kumar, S.A., Alhamami, M.A., Almehbad, N. and Algadi, H., **2024**. Exploring the potential of reduced graphene oxide/polyaniline (rGO@ PANI) nanocomposites for high-performance supercapacitor application. *Electrochimica Acta*, 479, p.143743.
- [6] Umar, A., Jung, I., Ibrahim, A.A., Akhtar, M.S., Kumar, S.A., Alhamami, M.A., Almas, T., Almehbad, N. and Baskoutas, S., **2024**. Porous Mn<sub>2</sub>O<sub>3</sub> nanorods-based electrode for high-performance electrochemical supercapacitor. *Journal of Energy Storage*, 81, p.110305.
- [7] Umar, A., Raut, S.D., Ibrahim, A.A., Algadi, H., Albargi, H., Alsaiani, M.A., Akhtar, M.S., Qamar, M. and Baskoutas, S., **2021**. Perforated Co<sub>3</sub>O<sub>4</sub> nanosheets as high-performing supercapacitor material. *Electrochimica Acta*, 389, p.138661.
- [8] H. Zhou, M. Ren, H.-J. Zhai, **2021**. Enhanced supercapacitive behaviors of poly (3,4-ethylenedioxythiophene)/ graphene oxide hybrids prepared under optimized electropolymerization conditions. *Electrochimica Acta* 372, pp. 137861.
- [9] Umar, A., Akhtar, M.S., Ameen, S., Imran, M., Kumar, R., Wang, Y., Ibrahim, A.A., Albargi, H., Jalalah, M., Alsaiani, M.A. and Al-Assiri, M.S., **2021**. Colloidal synthesis of NiMn<sub>2</sub>O<sub>4</sub> nanodisks decorated reduced graphene oxide for electrochemical applications. *Microchemical Journal*, 160, p.105630.
- [10] X. Li, A.M. Elshahawy, C. Guan, J. Wang, **2017**. Metal phosphides and phosphates-based electrodes for electrochemical supercapacitors, *Small* 13, pp.1701530.
- [11] J. Theerthagiri, R.A. Senthil, P. Nithyadharseni, S.J. Lee, G. Durai, P. Kuppusami, J. Madhavan, M.Y. Choi, **2020**. Recent progress and emerging challenges of transition metal sulfides based composite electrodes for electrochemical supercapacitive energy storage. *Ceramics International*. 46, pp.14317–14345.
- [12] L. Zhang, S. Zheng, L. Wang, H. Tang, H. Xue, G. Wang, H. Pang, **2017**. Fabrication of metal molybdate micro/nanomaterials for electrochemical energy storage. *Small* 13, pp.1700917.
- [13] Kamble, T.P., Shingte, S.R., Chavan, V.D., Kim, D. K., Chougale, A.D., Dongale, T.D. and Patil, P.B. **2024**. MOF Derived CoFe<sub>2</sub>O<sub>4</sub>@Carbon Nanofibers for Supercapacitor Application. *ChemSci Advances* 1(1), pp. 34-40.
- [14] L. Shen, L. Yu, H. Bin Wu, X.Y. Yu, X. Zhang, X.W. Lou, **2015**. Formation of nickel cobalt sulfide ball-in-ball hollow spheres with enhanced electrochemical pseudocapacitive properties, *Nature Communications*. 6, pp.1–8.
- [15] V. Gajraj, C.R. Mariappan, **2020**. Electrochemical performances of asymmetric aqueous supercapacitor based on porous Cu<sub>3</sub>Mo<sub>2</sub>O<sub>9</sub> petals and La<sub>2</sub>Mo<sub>3</sub>O<sub>12</sub> nanoparticles fabricated through a simple coprecipitation method. *Applied Surface Science* 512, pp.145648.

- [16] D. Guo, Y. Luo, X. Yu, Q. Li, T. Wang, **2014**. High performance NiMoO<sub>4</sub> nanowires supported on carbon cloth as advanced electrodes for symmetric supercapacitors, *Nano Energy* 8, pp.174–182.
- [17] X. Hu, W. Zhang, X. Liu, Y. Mei, Y. Huang, **2015**. Nanostructured Mo-based electrode materials for electrochemical energy storag. *Chemical Society Review*. 44, pp.2376–2404.
- [18] Z.X. Yin, S. Zhang, Y.J. Chen, P. Gao, C.L. Zhu, P.P. Yang, L.H. Qi, **2015**. Hierarchical nanosheet-based NiMoO<sub>4</sub> nanotubes: synthesis and high supercapacitor performance. *Journal of Materials Chemistry A* 3, pp.739–745.
- [19] K. Seevakan, A. Manikandan, P. Devendran, Y. Slimani, A. Baykal, T. Alagesan, **2018**. Structural, morphological and magneto-optical properties of CuMoO<sub>4</sub> electrochemical nanocatalyst as supercapacitor electrode. *Ceramics International* 44 , pp.20075–20083,
- [20] G.K. Veerasubramani, K. Krishnamoorthy, S. Radhakrishnan, N.J. Kim, S.J. Kim, **2014**. Synthesis, characterization, and electrochemical properties of CoMoO<sub>4</sub> nanostructures. *International Journal of Hydrogen Energy* 39, pp.5186-5193.
- [21] Y.-P. Gao, K.-J. Huang, C.-X. Zhang, S.-S. Song, X. Wu, **2018**. High-performance symmetric supercapacitor based on flower-like zinc molybdate. *Journal of Alloys Compounds* 731, pp.1151-1158.
- [22] D. Cai, D. Wang, B. Liu, Y. Wang, Y. Liu, L. Wang, H. Li, H. Huang, Q. Li, T. Wang, **2013**. Comparison of the electrochemical performance of NiMoO<sub>4</sub> nanorods and hierarchical nanospheres for supercapacitor applications. *ACS Applied Materials and Interfaces* 5, pp.12905-12910.
- [23] Ge, Jinhua, Jihuai Wu, Leqing Fan, Quanlin Bao, Jia Dong, Jinbiao Jia, Yaoqi Guo, and Jianming Lin. **2018**. "Hydrothermal synthesis of CoMoO<sub>4</sub>/Co<sub>1-x</sub>S hybrid on Ni foam for high-performance supercapacitors." *Journal of Energy Chemistry* 27(2), pp. 478-485.
- [24] Z. Zhang, Y. Liu, Z. Huang, L. Ren, X. Qi, X. Wei, J. Zhong, **2015**. Facile hydrothermal synthesis of NiMoO<sub>4</sub>@CoMoO<sub>4</sub> hierarchical nanospheres for supercapacitor ap plications. *Physical Chemistry Chemical Physics*. 17, pp.20795–20804.
- [25] Z. Yin, Y. Chen, Y. Zhao, C. Li, C. Zhu, X. Zhang, **2015**. Hierarchical nanosheet-based CoMoO<sub>4</sub>-NiMoO<sub>4</sub> nanotubes for applications in asymmetric supercapacitors and the oxygen evolution reaction. *Journal of Materials Chemistry A* 3, pp. 22750–22758.
- [26] Gopi, Chandu VV Muralee, Sangaraju Sambasivam, Kummara Venkata Guru Raghavendra, Rajangam Vinodh, Ihab M. Obaidat, and Hee-Je Kim. **2020**. Facile synthesis of hierarchical flower-like NiMoO<sub>4</sub>-CoMoO<sub>4</sub> nanosheet arrays on nickel foam as an efficient electrode for high-rate hybrid supercapacitors. *Journal of Energy Storage* 30, pp. 101550.
- [27] Zhang, Ziqing, Hongdan Zhang, Xinyang Zhang, Deyang Yu, Ying Ji, Qiushi Sun, Ying Wang, and Xiaoyang Liu. **2016**. Facile synthesis of hierarchical CoMoO<sub>4</sub>@ NiMoO<sub>4</sub> core-shell nanosheet arrays on nickel foam as an advanced electrode for asymmetric supercapacitors. *Journal of Materials chemistry A* 4(47), pp.18578-18584.
- [28] Khadka, Ashwin, Edmund Samuel, Bhavana Joshi, Yong Il Kim, Ali Aldabahi, Mohamed El-Newehy, Hae-Seok Lee, and Sam S. Yoon. **2023**. Bimetallic CoMoO<sub>4</sub> Nanosheets on Freestanding Nanofiber as Wearable Supercapacitors with Long-Term Stability. *International Journal of Energy Research* 2023(1), pp. 2910207.
- [29] Fan, Jiahui, Xin Chang, Lu Li, and Mingyi Zhang. **2023**. Synthesis of CoMoO<sub>4</sub> nanofibers by electrospinning as efficient electrocatalyst for overall water splitting. *Molecules* 29(1), pp. 7.
- [30] Chang, Liang, Shaoqin Chen, Yuhuan Fei, Dario J. Stacchiola, and Yun Hang Hu. **2023**. Superstructured NiMoO<sub>4</sub>@CoMoO<sub>4</sub> core-shell nanofibers for supercapacitors with ultrahigh areal capacitance. *Proceedings of the National Academy of Sciences* 120 (12), pp. e2219950120.
- [31] J. L. Patil, R. A. Chavan, A. S. Sutar, S. S. Kulkarni, R. K. Dhanvade, P. B. Patil, S. R. Shingte, S. J. Pawar. **2025**. Electrodeposited MnO<sub>2</sub> Thin Film as High Performance Electrode for Supercapacitor Application. *SciEngg Advances*, 2(1), pp.16-25.
- [32] Sahoo, Surjit, Karthikeyan Krishnamoorthy, Parthiban Pazhamalai, and Sang-Jae Kim. **2018**. Copper molybdenum sulfide anchored nickel foam: a high performance, binder-free, negative electrode for supercapacitors. *Nanoscale* 10 (29), pp.13883-13888.
- [33] Wu, Liping, Xincun Tang, Xi Chen, Zhihao Rong, Wei Dang, Yang Wang, Xing Li, Liuchun Huang, and Yi Zhang. **2020**. Improvement of electrochemical reversibility of the Ni-Rich cathode material by gallium doping. *Journal of Power Sources* 445, pp.227337.

- [34] Zhao, Yunxuan, Fei Teng, Zailun Liu, Qian Du, Jingjing Xu, and Yiran Teng. **2016**. Electrochemical performances of asymmetric super capacitor fabricated by one-dimensional CoMoO<sub>4</sub> nanostructure. *Chemical Physics Letters* 664, pp. 23-28.
- [35] Zhang, Y., Chang, C.R., Jia, X.D., Cao, Y., Yan, J., Luo, H.W., Gao, H.L., Ru, Y., Mei, H.X., Zhang, A.Q. and Gao, K.Z., **2020**. Influence of metallic oxide on the morphology and enhanced supercapacitive performance of NiMoO<sub>4</sub> electrode material. *Inorganic Chemistry Communications*, 112, p.107697.
- [36] Zhang, Yong, Cui-rong Chang, Xiao-dong Jia, Qing-yuan Huo, Hai-li Gao, Ji Yan, Ai-qin Zhang et al. **2020**. "Morphology-dependent NiMoO<sub>4</sub>/carbon composites for high performance supercapacitors." *Inorganic Chemistry Communications* 111, pp. 107631.
- [37] Mai, Li-Qiang, Fan Yang, Yun-Long Zhao, Xu Xu, Lin Xu, and Yan-Zhu Luo. **2011**. "Hierarchical MnMoO<sub>4</sub>/CoMoO<sub>4</sub> heterostructured nanowires with enhanced supercapacitor performance." *Nature Communications* 2(1), pp. 381.
- [38] Nti, Frederick, Daniel Adjah Anang, and Jeong In Han. **2018**. "Facilely synthesized NiMoO<sub>4</sub>/CoMoO<sub>4</sub> nanorods as electrode material for high performance supercapacitor." *Journal of Alloys and Compounds* 742, pp. 342-350.
- [39] Hussain, Shahid, Abdul Jabbar Khan, Muhammad Arshad, Muhammad Sufyan Javed, Awais Ahmad, Syed Shoaib Ahmad Shah, Mohammad Rizwan Khan et al. **2021**. "Charge storage in binder-free 2D-hexagonal CoMoO<sub>4</sub> nanosheets as a redox active material for pseudocapacitors." *Ceramics International* 47 (6), pp.8659-8667.
- [40] Seevakan, K., A. Manikandan, P. Devendran, Y. Slimani, A. Baykal, and T. Alagesan. **2018**. "Structural, morphological and magneto-optical properties of CuMoO<sub>4</sub> electrochemical nanocatalyst as supercapacitor electrode. *Ceramics International* 44 (16), pp. 20075-20083.
- [41] Guo, Di, Haiming Zhang, Xinzhi Yu, Ming Zhang, Ping Zhang, Qihong Li, and Taihong Wang. **2013**. "Facile synthesis and excellent electrochemical properties of CoMoO<sub>4</sub> nanoplate arrays as supercapacitors." *Journal of Materials Chemistry A* 1 (24), pp.7247-7254.